Appl. Phys. B 29, 79–87 (1982)

Applied Physics B Photophysics and Laser Chemistry

© Springer-Verlag 1982

Low Threshold Optical Bistability with Optical Pumping

F. T. Arecchi*, G. Giusfredi, E. Petriella**, and P. Salieri
Istituto Nazionale di Ottica, I-50125 Firenze, Italy

Received 26 May 1982/Accepted 3 July 1982

Abstract. By use of circularly polarized light we have exploited optical pumping within the Zeeman sublevels of the ground state to obtain optical bistability in sodium vapours with low threshold power (around 1 mW) and a wide tuning range (>12 GHz). Experimental results are presented for different conditions of operation and compared to computer calculations, that include propagation effects and inhomogeneous broadening, based on a three-level atomic model that accounts for optical pumping.

PACS: 42.50, 42.65, 42.80

We report on experimental evidence of a new type of optical bistability (OB), based on optical pumping of the ground state sublevels of atomic Na. This OB is based on a drastic modification of the polarizability of the absorbing transition by massive transfer of the population into a "storage" level, thus requiring a reduced threshold intensity with respect to the usual saturation bleaching of a two-level system.

OB in a Fabry-Perot (FP) interferometer filled with Na vapour as a nonlinear transmission medium was demonstrated by Gibbs et al. [1]. By use of linearly polarized light tuned on the $D2$ line, they reported observation of dispersive OB [2], which arises from the interplay between cavity mistuning and atomic detuning with respect to the impinging frequency [3]. The nonlinearity in the index of refraction was provided by hyperfine pumping between the $F=1$ and $F=2$ degenerate sublevels of the ground state.

Shortly later theoretical interest was triggered by the analogy of OB with a thermodynamic first-order phase transition developed on the basis of Maxwell-Bloch equations for a medium of two-level atoms [4]. The initial theory was developed for absorbing OB in a resonant atom-field interaction and later extended to account for atom-field detuning and field cavity mistuning with all the atoms of the absorber supposed to experience the same (mean) field [5]. This requires low single-pass absorption and high cavity finesse. This analysis was followed by a treatment for dispersive OB with inhomogeneous broadening that accounts for propagation effects [6].

With use of the $D1$ line in atomic sodium in a focusing FP cavity Sandle and Gallagher [7] tried to provide experimental comparisons with the above two-level model by substantial collisional broadening at high laser power. Again linearly polarized light was used and the observed OB was mainly dispersive. Clear evidence of absorptive OB was obtained in a Doppler-free experiment that made use of multiple atomic Na beams [8] orthogonal to the laser radiation.

In the presence of a two-level absorber, to modify the linear susceptibility the local field E must be of the order of the saturation value $E_s=(\hbar/\mu)(\gamma_\perp\gamma_s)^{1/2}$, where μ is the electric dipole matrix element, $\gamma_\perp$ the dipole decay rate, and γ_s the excited upper level population decay rate due to spontaneous emission.

In atomic sodium, by application of a weak magnetic field, the ground state spins can be aligned collinearly with the direction of propagation of the laser-light beam. At the $D1$ line then, with circularly polarized radiation, optical pumping takes place. This implies a depletion of the levels coupled to the upper optical state by the selected circular polarization, thus modifying the susceptibility of the absorber. For instance, if we apply σ_+ polarization the selection rule

* Also University of Florence
** On leave from CEILAP, Buenos Aires, Argentina

0721-7269/82/0029/0079/$01.80

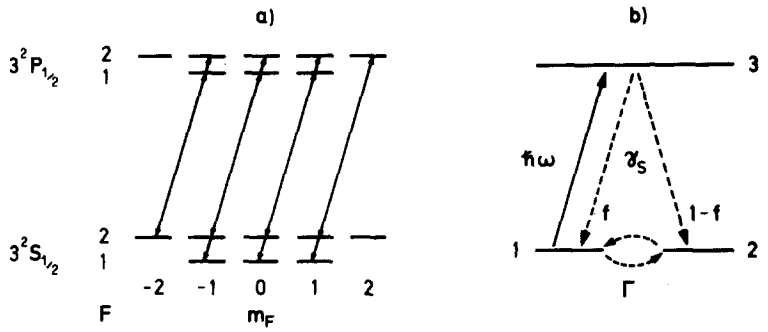

Fig. 1. (a) Zeeman structure and allowed transitions of Na under illumination with σ_+ polarized radiation tuned at the $D1$ line. (b) Three level simplified model for interaction with circularly polarized radiation

$\Delta m = +1$ couples the $m_f = -2$ to $m_f = +1$ sublevels of the Na ground state with the excited state, whereas $m_f = +2$ remains uncoupled. At intensity levels such that the induced transition rate is lower than the spontaneous one, spontaneous emission overfills the $m_f = +2$ state at the expense of the other ones, thus making the vapour partly transparent to the σ_+ radiation. In this case the effective saturation requirement becomes $E > E_s^* = (h/\mu)(\gamma_\perp \Gamma)^{1/2}$, with Γ of the order of the relaxation rate τ_1^{-1} between the populations of the uncoupled $m_f = +2$ level and the manifold of the other m_f levels of the ground state. The relaxation time τ_1 for ground state spin orientation is much longer than the excited state spontaneous decay time. With respect to the ordinary two-level case, this implies a substantial reduction of the saturation power by a factor Γ/γ_s [9]. By exploitation of optical pumping within the Zeeman sublevels of the ground state of atomic Na we have observed OB with low threshold power (around 1 mW) and a wide tuning range (more than 12 GHz). The experimental results can be explained within the framework of a model that accounts for optical pumping and for the substantial Doppler broadening.

In Sect. 1 we discuss a simplified three-level model accounting for optical pumping. By this model we assume polarizability to be inserted as a source term in a field equation including propagation effects and inhomogeneous broadening. Section 2 and 3 describe the experimental setup and the experimental results. In Sect. 4 we fit these results with computer plots derived from our model.

1. The Three-Level Atomic Model

Optical pumping with laser irradiation is investigated in a three-level system. The analysis is based on the density matrix formalism in close analogy to the standard two-level case. The electric field, circularly polarized and propagating along the axis of the cavity can be written as

$$\mathbf{E}(t) = \mathbf{e}\frac{E_0}{2}\exp(i\omega t) + \text{c.c.} \tag{1}$$

with $\mathbf{e}$ representing the unit vector for the chosen circular polarization. We show in Fig. 1a the transitions allowed in atomic sodium under illumination with σ_+ circularly polarized radiation, for which the selection rule $\Delta m = +1$ applies, for the various components of the $D1$ manifold. Under weak laser excitation and low collisional broadening by Ar buffer gas, the atomic behaviour is complex and with linearly polarized light the absorption spectrum exhibits two prominent hyperfine components, each broadened by the Doppler effect. However, in the presence of a buffer gas, the effect of collisions is such that the upper state sublevels are mixed very rapidly [10] while the ground state sublevels population distribution is practically unaffected [11]. In the presence of circularly polarized light, we can consider the radiatively coupled manifold of the ground state as a single level, that we label as 1, indicating with 2 the uncoupled $m_f = +2$ ground-state sublevel and 3 the excited upper state. Atomic sodium is therefore modeled as in Fig. 1b, levels 1 and 3 interacting with the optical wave through the allowed electric dipole interaction

$$H' = -\mu_{13}E(t). \tag{2}$$

The excited level 3 decays through spontaneous emission to level 1 and 2, with branching ratios f and $1-f$, respectively. After absorbing a pump photon at the 1–3 transition, the atom can either return to state 1 or decay to state 2, so that the applied field will cause atoms initially in level 1 to accumulate in level 2. Absorption of resonant radiation by the vapour and its fluorescence will decrease as the sublevels that make up for level 1 in our simplified model are progressively depleted. However, this process cannot continue indefinitely as collisions tend to re-equilibrate the populations within the ground state. The balance reached between laser population transfer and relaxation gives rise, for a fixed intensity, to a steady-state population distribution with a given degree of orientation.

When a weak magnetic field, interacting with the magnetic moment of the atoms, is applied collinearly

to the beam axis, inducing a Zeeman splitting much smaller than the width of the $D1$ line, the pumping process follows the above given scheme.

In the absence of applied field, the occupation probabilities are 7/8 for level 1, 1/8 for level 2 and zero for the excited state. We take the fractional probability f to be equal to 7/8, as given by the degeneracy ratio. With these assumptions, the radiative interaction being described by the Rabi flopping frequency

$$\alpha = \frac{\mu_{13} E_0}{2\hbar} \tag{3}$$

the equation of motion for the density matrix in the interaction representation is

$$i\hbar \frac{\partial \varrho}{\partial t} = [\mathscr{H}_I', \varrho] + \text{relaxation terms}, \tag{4}$$

where $\mathscr{H}_I'$ is the Hamiltonian $\mathscr{H}'$ in the interaction representation. The components of (4) can be written as follows[1]

$$\dot{\varrho}_{11} = i(\alpha \varrho_{31} - \alpha^* \varrho_{13}) - (\varrho_{11}/7 - \varrho_{22})/\tau_1 + 7\varrho_{33}/8T_1, \tag{4a}$$

$$\dot{\varrho}_{22} = (\varrho_{11}/7 - \varrho_{22})/\tau_1 + \varrho_{33}/8T_1, \tag{4b}$$

$$\dot{\varrho}_{33} = -i(\alpha \varrho_{31} - \alpha^* \varrho_{13}) - \varrho_{33}/T_1, \tag{4c}$$

$$\dot{\tilde{\varrho}}_{13} = -i\alpha(\varrho_{11} - \varrho_{33}) - i\left(\bar{\Delta} - \frac{i}{T_2}\right)\tilde{\varrho}_{13}, \tag{4d}$$

where a rapidly oscillating factor in the off-diagonal element has been removed with the definition

$$\varrho_{13} = \tilde{\varrho}_{13} \exp(i\omega t) \tag{5}$$

and where $\bar{\Delta}$ is the atomic detuning $\omega - \omega_{13}$. We have denoted by T_2 the decay time of the optical coherence ϱ_{13} and T_1 the total spontaneous relaxation time from the excited state. We shall indicate the reciprocal of these relaxation times by $\gamma_\perp$ and γ_s, respectively. The time scales are such that $\gamma_\perp > \gamma_s \gg 1/\tau_1$. Defining the polarization $S = iN\varrho_{13}$ and solving (4) for the steady state we obtain

$$S = \frac{7\alpha N}{8\gamma_\perp} \frac{1 - i\Delta}{1 + \Delta^2 + 4|\alpha|^2/\Gamma\gamma_\perp} \tag{6}$$

indicating with $\Delta = (\omega - \omega_{13})/\gamma_\perp$ the atomic detuning normalized to the half-width homogeneous line and with N the number of atoms. In the last expression we have defined Γ so that

$$1/\Gamma = 15/16\gamma_s + 7\tau_1/128. \tag{7}$$

[1] During completion of this experiment a similar level scheme has been proposed for OB [12]. However that physics is substantially different, insofar as that paper considers equal matrix elements for the transitions 1–3 and 2–3, and hence it is missing the idea of a strong selection rule and consequent optical pumping which yields the low threshold power

For a two level system (1 indicates the lower and 2 the upper state) characterized by the rates $\gamma_s = 1/T_1$ and $\gamma_\perp = 1/T_2$, the polarization $S = iN\varrho_{12}$ is easily obtained as

$$S = \frac{\alpha N}{\gamma_\perp} \frac{1 - i\Delta}{1 + \Delta^2 + 4|\alpha|^2/\gamma_s\gamma_\perp}. \tag{8}$$

We see then that the net effect of optical pumping with circular polarization is the replacement, in the intensity dependent saturation term, of the factor $1/\gamma_s$ with $1/\Gamma \sim 7\tau_1/128$, and the multiplication by 7/8 arising from the ground state degeneracy. At the argon buffer gas pressures that have been used the Doppler width (~ 1.6 GHz) is considerably broader than $\gamma_\perp (\gamma_\perp = \gamma_s/2 + 2\pi \cdot 10^7 \cdot p \cdot s^{-1}$, with p the Argon pressure measured in Torr [13]) and the line is essentially inhomogeneous in character.

The coupling of the excited system with the field is described by the Maxwell equation for the slowly varying envelope of the electric field E

$$\frac{\partial E}{\partial t} + c\frac{\partial E}{\partial z} = -g \int S_\omega d\omega, \tag{9}$$

where according to (6)

$$S_\omega = \frac{7\alpha N(\omega)}{8\gamma_\perp} \frac{1 - i\Delta}{1 + \Delta^2 + 4|\alpha|^2/\Gamma\gamma_\perp} \tag{10}$$

is the polarization associated with the isochromat of angular frequency ω, $N(\omega)d\omega$ being the number of atoms with resonant frequency between ω and $\omega + d\omega$ so that $\int N(\omega)d\omega = N$. The coupling constant g is given by

$$g = \omega\mu_{13}/\varepsilon_0 V \tag{11}$$

with V the volume of the atomic sample.

The field equation must be supplemented by the proper boundary conditions. At the operating temperature the sodium cell is not optically thin, so that the mean field analysis for OB in a FP interferometer [5] cannot be applied. In order to obtain an analytical exact solution the inhomogeneous line shape is taken as Lorentzian. For the sake of computation we consider the atomic system placed in a ring cavity. In fact, with Doppler inhomogeneous broadening in a gaseous medium, the analysis in a FP interferometer is complicated by the presence of both forward and backward waves and hence simultaneous positive and negative frequency shifts. Calculations carried out including standing-wave effects [14, 15] do not indicate major quantitative differences with respect to the ring analysis. For instance, in the case of a homogeneously broadened line, switching power have been calculated to be a factor 1/3 lower [16]. Even smaller deviations are expected for an inhomogeneous line. This factor is within the range of error in the guess

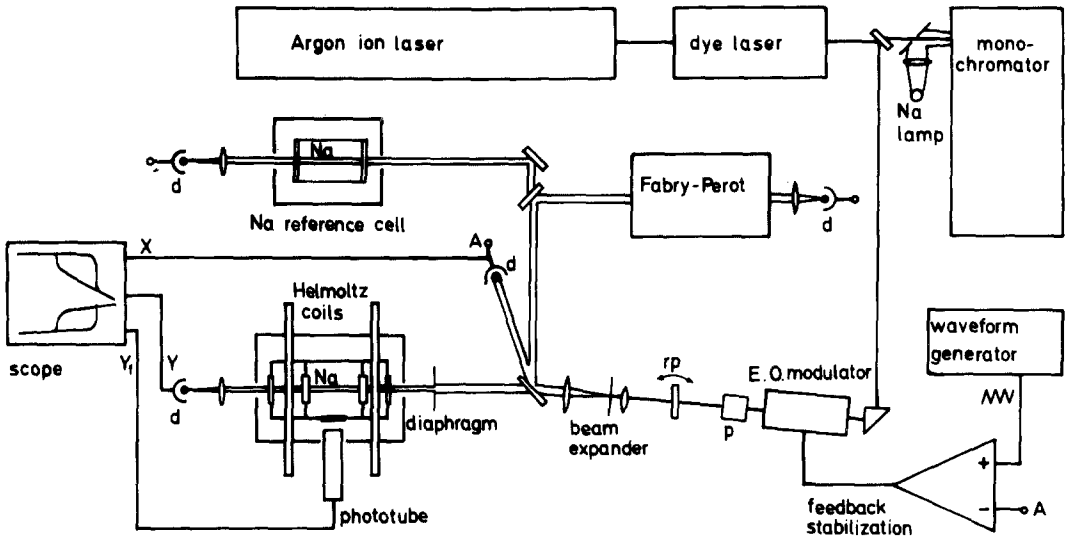

Fig. 2. The experimental arrangement. (A: feedback signal, d: detector, p: polarizer, rp: retardation plate)

of the proper value of τ_1, which, by virtue of (6), determines the required saturation power. With these considerations, we just have to replace our three-level polarizability (6) instead of the two-level one (8) into [Ref. 6, Eqs. (14)–(16)] in order to develop a numerical calculation.

2. Experimental Set-Up

A schematic of the experimental arrangement is shown in Fig. 2. A Coherent 599-21 dye laser with Rhodamine 6 G pumped by an argon laser has been used. The single-mode feedback-locked output presented a jitter of less than ± 1 MHz. The laser frequency was first roughly tuned to the $D1$ line with use of a monochromator and a reference sodium lamp, then finely and reproducibly tuned on the peak of the $F=2$ transition by monitoring the absorption of a sodium cell in a different oven kept at the same temperature as the OB cavity. We measured the laser frequency by scanning from this position with a temperature stabilized Burleigh Fabry-Perot interferometer. In fact, the laser was frequency stabilized with its own reference cavity, but at times, when scanning over a large interval of frequencies, it presented a hysteresis of about 100 MHz of mechanical origin in the mounting of the Brewster angle tuning plate. Therefore to accurately assess the emission frequency we decided to supplement the digital frequency readout provided by the laser control module with the indication of the interferometer. The laser intensity was modulated and stabilized through an E–O Pockels modulator driven by the signal of a photodiode in a feed-back loop. This servo system cut intensity fluctuations down to 1%. The modulation bandwidth available was dc to 500 kHz, but we generally modulated from 0 to 80% the laser power with a triangular wave at low frequencies, typically about 5 Hz, carefully avoiding subharmonics of the line. The beam was then circularly polarized by a quarter wave plate. This system also worked as an isolator preventing instabilities from feeding back reflections from the bistable device or the reference interferometer.

Before entering the OB cell the beam was spatially filtered with a pinhole and expanded to a diameter of about 4 mm. We could then vary its size in front of the OB device through a variable diaphragm. The OB device consisted of a carefully designed vacuum sealed stainless steel cell with internal mirrors that formed a FP interferometer. We must avoid Brewster windows to keep the polarization (Fig. 3). The main technical problem (exposure of multilayer coatings to Na vapours) was solved by mounting the mirrors with reflecting layers outward. Na vapours were confined within the central part of the cell that acted as cavity. The cell was further closed by AR coated end windows, with both end sides communicating with each other and connected to a valve in order to vary the buffer gas pressure. In fact the mirrors are mounted in their holders so as to undergo no deformation and leave a small leak to compensate pressure in the central chamber for the buffer gas. The small sodium quantity that might diffuse through this leak finds a way out in the tubes taking to the valve, which is kept at room temperature. Therefore the Na density outside the middle chamber is negligible and thus does not contribute to absorption of the laser beam. The

sodium reservoir was contained in the "cold finger", a glass tube at the bottom of the central chamber, whose temperature was kept a few degrees lower than the rest of the structure. Two different ovens stabilized within 1 degree °C the temperature both of the cell and of the cold finger, so as to control the Na vapour density and prevent Na condensation on the AR coating layers of the mirrors.

Stable alignment and fine tuning of the cavity was provided by deformable bellows and three suitable spacers and piezos. The mirrors, 25 mm in diameter and 7 mm thick, had each a reflectivity of about 96% with a 0.2% reflectivity residual for the AR coating. The finesse was about 30. The optical transmission of the properly tuned cavity without sodium vapour was about 20%. This can be attributed to non flatness of the mirror surfaces and small sodium deposits on the mirrors.

In the construction of the cell, particular care was taken to avoid the use of ferromagnetic materials. The cavity was in fact placed in between a pair of Helmholtz coils, 60 cm of diameter, with axis along the light beam, putting out a weak magnetic field of a few Gauss, so as to align the ground state spins.

Finally the transmitted and incident intensities were displayed as vertical and horizontal deflections on an oscilloscope. We also displayed the fluorescent intensity as detected with a photomultiplier through a lateral window orthogonally to the beam direction.

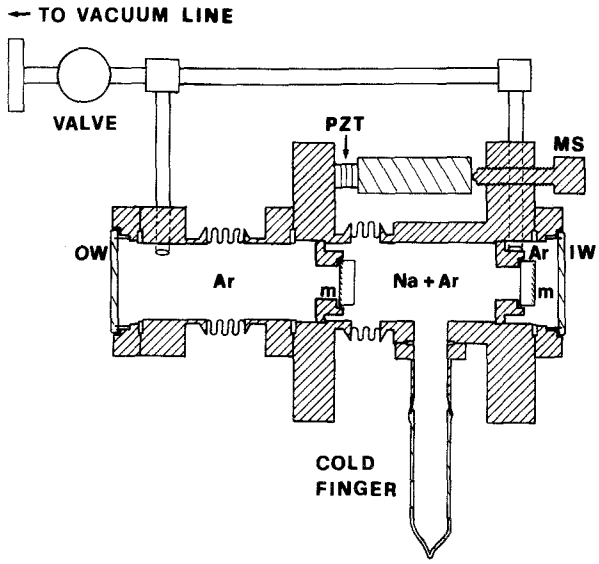

Fig. 3. Schematic of the sodium filled FP interferometer, (MS: micrometric screw, m: mirror, IW: input window, OW: output window)

3. Experimental Results

By looking at the transmission of sodium vapours with circularly polarized light without cavity mirrors we could establish the presence of nonlinearity and the availability of sufficient light intensity ($\sim$1 mW) to observe it. This test confirmed the power requirements for laser Zeeman pumping quoted in [17]. With the mirrors inserted, bistable curves were observed on peaking up the finesse through the piezo controls. They were then photographed as monitored on the scope. The free spectral range of the FP interferometer constituting the bistable device was 1.45 GHz, which accounting for the mirror thickness, corresponds to 8.24 cm length for the absorbing region.

We scanned the laser in frequency over an interval many times broader than the atomic resonance width, thereby investigating the effects associated with atomic detuning. Cavity mistuning was investigated by shifting the laser frequency of a fixed amount, comparable with the empty cavity bandwidth, always returning to the initial zero mistuning position reoptimizing the transmission. The influence of collisional broadening was examined by varying the argon buffer gas pressure in the 0–40 mbar range. In the absence of argon, bistability could be observed also with the weak external magnetic field turned off. We attribute this latter OB to hyperfine pumping as in the experiment of Gibbs et al. [1]. For most measurements the temperature of operation was kept at 180 °C. Knowledge of the temperature allowed us to determine the sodium vapour density with a 1% accuracy [18].

A summary of collected data is here shown followed by a discussion. In Fig. 4–8 we have collected the most relevant out of a large body of experimental data. Precisely, Fig. 4 shows the transmission function of the scanned sodium filled FP at different frequency detunings, as observed while measuring OB data. In Figs. 5–7 we show the OB hysteresis curves, that is output intensity versus input intensity as we recorded them by varying the mistuning, detuning and Argon pressure, respectively. Figure 8 shows another set of OB curves as monitored on the scope, including fluorescence intensity viewed orthogonally to the beam.

Bistability as observed is dispersive in character and the inhomogeneous line plays an important role to account for the phenomenology of the observed results. Indeed, as already stressed, even at the highest buffer gas pressures used, the collisional homogeneous width is less than one-third of the Doppler linewidth.

At zero laser detuning absorptive bistability is not seen, nor it is expected in these conditions [19]. Figure 4, taken with the FP in the scanning mode, clearly show that the origin of the bistable behaviour is

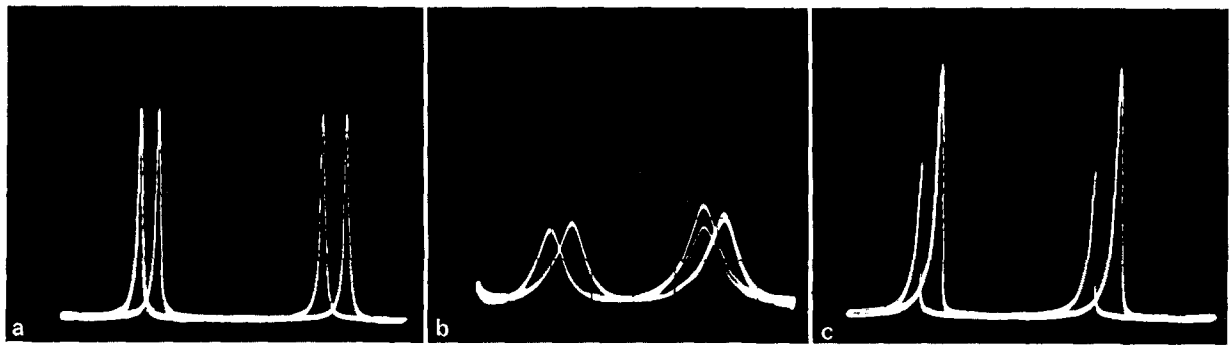

Fig. 4a–c. Transmission function of the FP in scanning mode. Input power 2 mW, temperature 183 °C, argon pressure: 15 Torr. (a) Away from resonance, peak cavity transmission (PCT) 22 %, (b) on resonance minimum transmission, PCT 2 %, (c) 2 GHz detuning from center of $D1$ doublet, PCT 11 %. Two curves appear due to hysteresis in the PZT scan. Cavity length increases to the left. PZT scan frequency 5 Hz

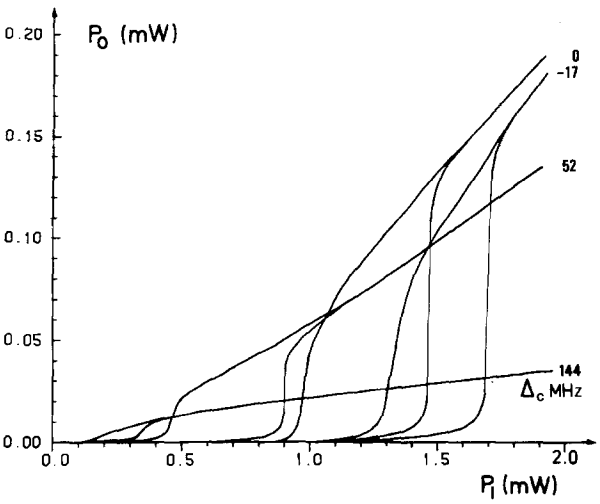

Fig. 5. Power out (P_0) *vs* power in (P_i) measured at constant detuning $\bar{\Delta} = +1.5$ GHz from the center of the $D1$ doublet for different cavity mistuning Δ_c values. Temperature 180 °C, argon pressure 26.5 Torr. Beam diameter 2 mm as for all the following figures

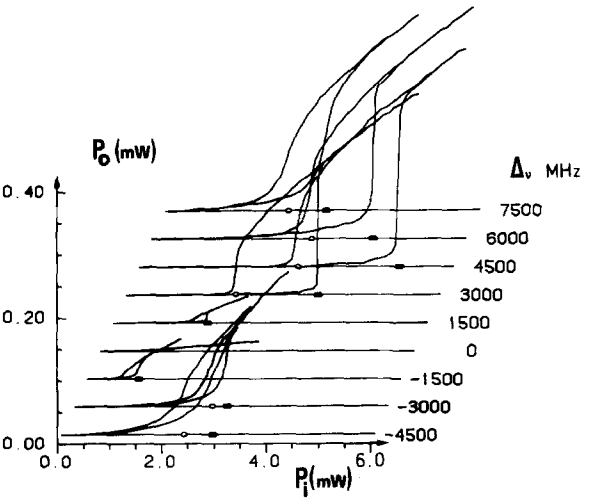

Fig. 6. Power out (P_0) vs power in (P_i) observed at different detuning values measured from the peak of the $F=2$ hyperfine transition (Fig. 1a). (Temperature: 180 °C, argon pressure: 16.5 Torr)

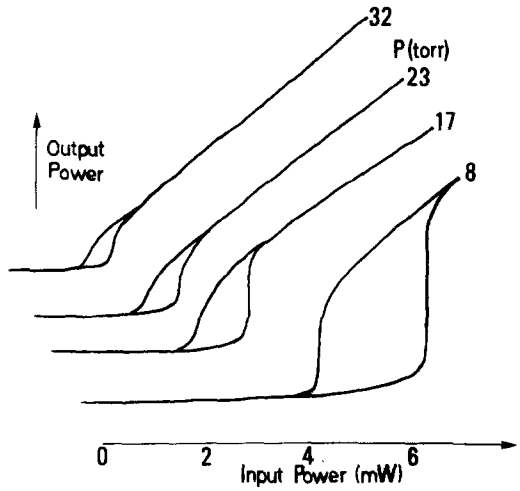

Fig. 7. Hysteresis curves at different values of argon pressure (p). (Temperature: 180 °C, detuning: 2.25 GHz)

dispersive. In these pictures, the direction of the asymmetry depends upon the sign of the nonlinear index and therefore reverses with detuning around resonance. We tuned the laser frequency over a large interval away from resonance and the FP outputs always remained asymmetric. Contrary to the case of Gibbs et al. [1] we do not observe any frequency at which the profiles are symmetric and the nonlinear index is zero. In our case this is so because, for any atomic velocity group, the backward running wave is not antagonist with the forward in the pumping mechanism which only goes from level 1 to level 2 (Fig. 1b) and not the other way round. This pumping mechanism brings about a much wider tuning range both in the allowed atomic detuning and cavity mistuning than in the case of [1] (Figs. 5 and 6).

In Fig. 7 we see how the addition of buffer gas lowers the bistability threshold and the histeresis loop width, by making the line more homogeneous. In Fig. 8 hysteresis is also shown in the fluorescence intensity as

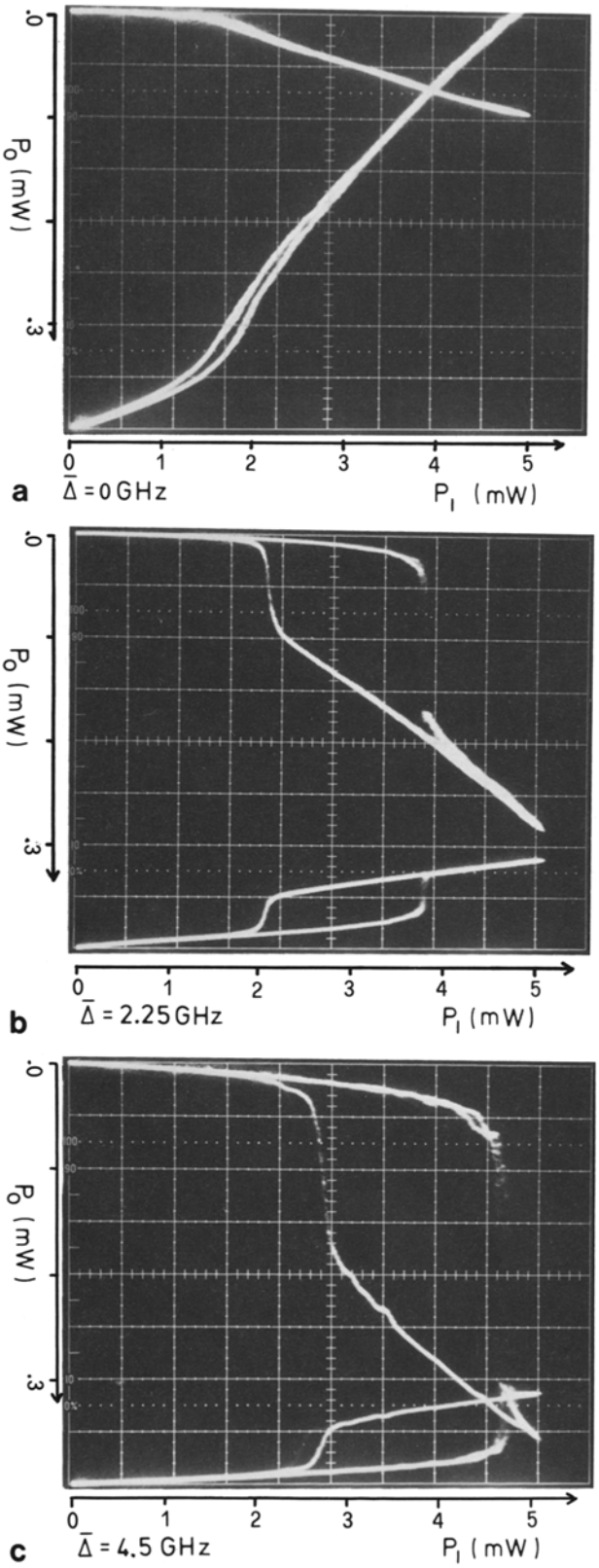

Fig. 8a–c. OB in transmission (top) and in fluorescence emission (bottom). (Temperature: 180 °C, argon pressure: 16.5 Torr, detuning in GHz from center $D1$ line indicated. P_i: power in, P_0: power out, fluorescence signal 1 V/div (a) and (c), 2 V/div (b)

viewed orthogonally to the beam. Though we operated at intensities considerably lower than those required to saturate the radiative transition (77 mW/cm^2 in absence of buffer gas [20] and about 20 times higher at the argon pressures we generally utilized), so that the stimulated emission rate is well below the spontaneous emission rate, the slow relaxation between levels 2 and 1 allows bleaching of the 1–3 transition at a much lower (a factor Γ/γ_s) intensity. Indeed, defining

$$X = 4|\alpha|^2/\gamma_\perp \Gamma \tag{12}$$

we easily obtain from (4)

$$\varrho_{33} = \frac{7\Gamma}{16\gamma_s} \frac{X}{1+\Delta^2+X}. \tag{13}$$

Fluorescence intensity monitors the occupation probability of the excited level 3. As in the two-level absorber case [5], we expect, past the hysteresis loop, fluorescence emission to level off with increasing input power. The input beam was circularly polarized with $\sim 2\%$ accuracy. We attribute the observed further increase in fluorescence with input intensity to this residual component of different polarization, that is absorbed by the vapour.

Finally, as in the case of [1] we have turn-on times in the range of 1–10 μs. Turn-off times are typically longer. This is so because the whole volume of the cell has been optically pumped in the meanwhile.

4. Comparison Between Theory and Experimental Data

Following the analysis outlined in Sect. 2 we solved numerically on a minicomputer [Ref. 6, Eqs. (14)–(16)], which yield, respectively, the single-pass dephasing $\varphi(L)-\varphi(0)$ over the cavity length L, the single pass field gain αL and the output versus input normalized field amplitudes. We remind that [6] accounts for propagation effects and inhomogeneous broadening and that we replaced in that theory the two-level polarizability with our three-level one. The calculations were performed for a variety of different parameter values, as they apply to our case, thus obtaining curves as those shown in Figs. 9–11. These have to be examined, respectively, with reference to the experimental results shown in Figs. 5–7, as they have been computed simulating the same experimental conditions. All the basic qualitative features of the observed results can be found. For the sake of clarity in the computer plots we have left the unstable negative slope branch without showing the resulting hysteresis cycle. This must be taken into account for comparison with the experimental data.

In our calculations we used $T_1 = 16$ ns [21], calculated T_2 as a function of argon pressure according to [13]

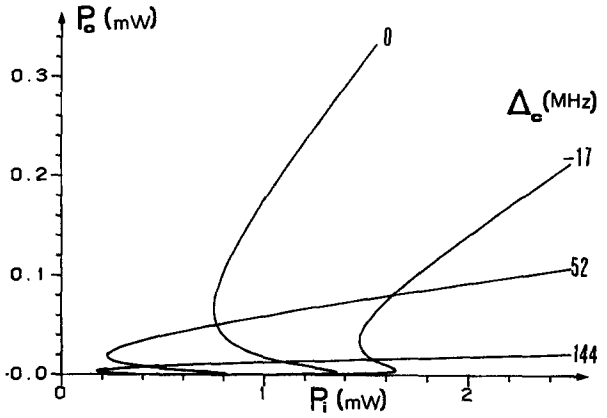

Fig. 9. Calculated transmission curves. Power out (P_0) is plotted vs power in (P_i). The cavity detuning Δ_c is varied as indicated. Argon pressure is taken as 26.5 Torr and τ_1 is assumed as 4.5 ms. As for Figs. 10 and 11 a nonsaturable absorption $A=0.04$ is assumed

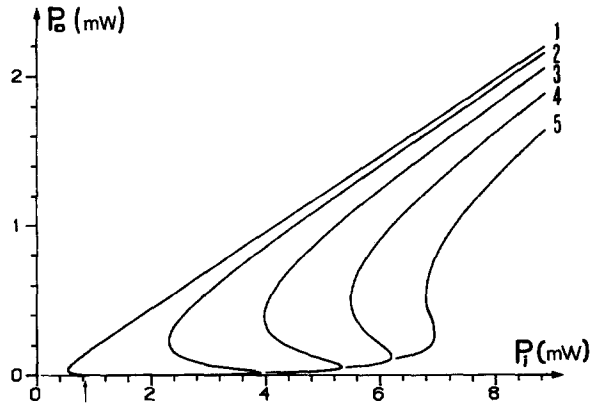

Fig. 10. Calculated transmission curves for different detuning (Δ) values. Cavity mistuning is taken as 0 MHz, argon pressure as 16.5 Torr, relaxation time τ_1 as 3.5 ms, temperature as 180 °C. Respectively, Δ is: *1* 0.5 GHz, *2* 2.5 GHz, *3* 4.5 GHz, *4* 6.5 GHz, *5* 8.5 GHz

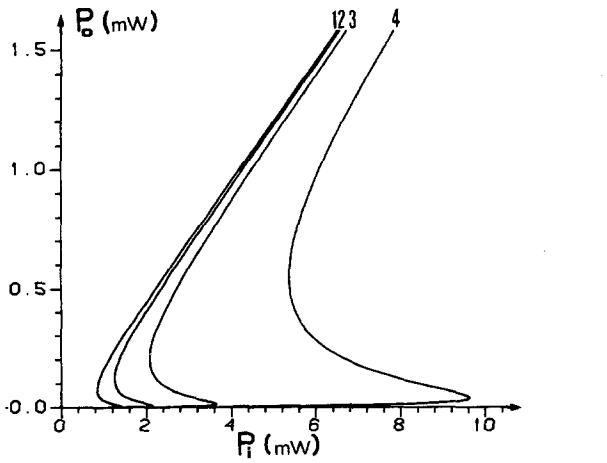

Fig. 11. Calculated transmission curves for different argon pressure (p). Temperature 180 °C, cavity mistuning 0 MHz, atomic detuning 2.25 GHz. Respectively, we take for p in Torr and for τ_1 in ms: *1* $p=32$, $\tau_1=5$, *2* $p=23$, $\tau_1=4.3$, *3* $p=17$, $\tau_1=3.5$, *4* $p=8$, $\tau_1=2.5$

and obtained both the inhomogeneous width and the absorber atomic density from the temperature. The ground state relaxation time τ_1 is known to be of the order of a few milliseconds. Relaxation times for Zeeman pumping are in fact very long [22]. In our case the basic limitation to optical pumping lies in the atomic collisions with the walls of the sodium cell, 4 cm in diameter, that have not been specially coated. A collision with the wall in fact brings about a random orientation in the spin of the outcoming atom. Therefore τ_1 is of the order of the time it takes for the atoms to diffuse from the center to the border of the cell. We then used for τ_1 a set of values that increase with the argon pressure, as diffusion is slowed, and that give an appropriate power scaling. It is important to notice that, within this model, the behaviour with laser frequency variations, for both detuning and cavity mistuning, is independent of the value of τ_1.

The input power is calculated assuming an incoming laser beam of 0.2 cm in diameter, as was experimentally the case. By inserting a diaphragm in front of the cell we have selected the central region of the collimated single TEM_{00} mode beam. Hence we have a spatially uniform intensity profile, less sensitive to transverse effects than it would be with a Gaussian distribution [23].

As can be seen from Fig. 6 a consistent degree of asymmetry has been observed in the hysteresis loops when scanning in frequency above and below resonance. This has no equivalent in our model calculation, as our analytical expressions are symmetric with frequency when the sign is changed for both the atomic detuning and the cavity mistuning.

Though we operate at very low intensities, we tentatively attribute this behaviour to a weak effect of resonant self-focusing that is enhanced by the cavity. Indeed, with an absorbing medium, nonlinearities in the index of refraction (the same that make a device such as ours work) result in focusing for frequencies above resonance and defocusing below it [24].

5. Conclusion

By building a Na cell which can be illuminated by circular polarization without consistently affecting the losses of the FP cavity we have observed OB due to optical pumping between the magnetic sublevels of the ground state.

The main result, justified in detail by a three-level approach, is that the stimulated transition rate $|\alpha|^2/\gamma_\perp$ has to be compared with an equivalent relaxation rate Γ between the two magnetic ground state levels rather than with the spontaneous rate of the optical transition γ_s, as in a two-level theory [4. 5] or with the hyperfine

pumping relaxation that is an order of magnitude faster [22], as in the case of experiment [1].

We have measured the OB hysteresis curves for different values of cavity mistuning, atomic detuning and buffer gas pressure. A numerical analysis fits qualitatively with the experiment, provided:

i) we introduce the three-level polarizability into a propagating field equations and account for inhomogeneous broadening,

ii) we currently use available numerical data for all parameters, with the exception of the ground state magnetic sublevels relaxation time τ_1 which results, by the fitting requirement, to be of a few milliseconds as expected,

iii) introduction of transverse self-focusing and defocusing effects leads to prediction of an asymmetry between positive and negative atomic detuning. This asymmetry is indeed present in our experimental data, but no numerical attempt to account for it has been performed, hence this effect is missing in our numerical calculation.

iv) In estimating the detuning values, we also neglected the hyperfine separation within level 1. This could be accounted by a properly weighted average over the sublevels. Our simplification is justified if we consider that inhomogeneous broadening is comparable in width with the hyperfine $F=1$ to $F=2$ splitting (1.77 GHz) and by the fact that the spectral region where OB is more clearly expected and observed is offset in frequency away from resonance by a larger amount.

Even though our setup is very unpractical as a device, it may be worth mentioning that we report the lowest threshold power this far for intrinsic OB in a FP device [Ref. 25, Fig. 8]. Exploitation of the rather slow relaxation process within the magnetic sublevels scales the time features from the microsecond to the millisecond regime, just making it easier to investigate dynamical characteristics related to the OB transition. This will be the object of further work.

Acknowledgements. Work partly supported by contract C.N.R.-I.N.O. We thank T. Haensch, F. Strumia, and A. Politi for helpful discussions during this work. We also thank S. Acciai and L. Albavetti for technical assistance in the construction of the OB cell.

References

1. H.M. Gibbs, S.L. McCall, T.N.C. Venkatesan: Phys. Rev. Lett. **36**, 1135 (1976)
2. As customary we refer to absorptive and dispersive OB according to its origin in the absorptive or dispersive part of the atomic polarizability
3. For the sake of clarity, we consistently call throughout this paper detuning the frequency offset between the field and the atomic resonance and mistuning the offset between the field and activity frequencies
4. R. Bonifacio, L.A. Lugiato: Opt. Commun. **19**, 172 (1976)
5. R. Bonifacio, L.A. Lugiato: Phys. Rev. A **18**, 1129 (1978)
   For a review of theoretical recent developments on OB see also *Optical Bistability*, ed. by C.M. Bowden, M. Ciften, H.R. Robl (Plenum Press, New York 1980) and *Dissipative Systems in Quantum Optics*, ed. by R. Bonifacio (Springer, Berlin, Heidelberg, New York 1981)
6. M. Gronchi, L.A. Lugiato: Opt. Lett. **5**, 108 (1980)
7. W.J. Sandle, A. Gallagher: Phys. Rev. A **24**, 207 (1981)
   W.J. Sandle: In *Laser Physics*, ed. by D.F. Walls, J.D. Harvey (Academic Press, New York 1980) p. 225
8. K.G. Weyer, H. Wiedermann, M. Rateike, W.R. MacGilliwray, P. Meystre, H. Walther: Opt. Commun. **37**, 426 (1981)
9. M.S. Feld, M.M. Burns, T.U. Kühl, P.G. Pappas, D.E. Murnick: Opt. Lett. **5**, 79 (1980)
10. R. Seiwert: Ann. Phys. (N.Y.) **18**, 54 (1956)
    J. Pitze, L. Krause: Can. J. Phys. **45**, 2671 (1967)
11. F. Strumia: Supplemento al Nuovo Cimento **26**, 355 (1968). For Zeeman pumping in the presence of a buffer gas see W. Happer: Rev. Mod. Phys. **44**, 169 (1972)
    A. Corney: *Atomic and Laser Spectroscopy* (Clarendon Press, Oxford 1977) p. 597
12. D.F. Walls, P. Zoller: Opt. Commun. **34**, 260 (1980)
13. D.G. McCartan, J.M. Farr: J. Phys. B **9**, 985 (1976)
    R.H. Chatham, A. Gallagher, E.L. Lewis: J. Phys. B **13**, L7 (1980)
14. G.P. Agrawal, H.J. Carmichael: Opt. Acta **27**, 661 (1980)
15. J.A. Hermann: Opt. Acta **27**, 159 (1980)
16. S.L. McCall, H.M. Gibbs: Opt. Commun. **33**, 335 (1980)
17. P. Bicchi, L. Moi, B. Zambon: Nuovo Cimento B **49**, 9 (1979)
18. N. Ioli, F. Strumia, A. Moretti: J. Opt. Soc. Am. **61**, 1251 (1971)
19. S.L. McCall: Phys. Rev. A **9**, 1515 (1974)
20. J.E. Bjorkholm, A. Ashkin: Phys. Rev. Lett. **32**, 129 (1974)
21. B.P. Kibble, G. Copley, L. Krause: Phys. Rev. **153**, 9 (1967)
22. A. Moretti, F. Strumia: Phys. Rev. A **3** (1971)
23. P.D. Drummond: IEEE J. QE-**17**, 301 (1981)
24. A. Javan, P.L. Kelley: IEEE J. QE-**2**, 470 (1966)
25. P.W. Smith, W.J. Tomlinson: IEEE Spectrum **18**, 6.26 (1981)

Note added in proof: A similar experimental set up has been recently worked out by Mlynek et al., to be presented at the XII. Int. Quantum Electronics Conference (Munich, 22–25 June 1982). From the Abstract however [Appl. Phys. B**28**, 135 (1982)] the physics seems different, since the applied magnetic field is perpendicular to the e.m. field propagation direction, whereas in our case it is parallel, as discussed in the paper.